Journal of the European Ceramic Society **19** (1999) 2449–2453

PII: S0955-2219(99)00133-8
0955-2219/99/$ - see front matter

Interpenetrating Al_2O_3-$TiAl_3$ Alloys Produced by Reactive Infiltration

F. Wagner,* D. E. Garcia, A. Krupp and N. Claussen

Advanced Ceramics Group, Technische Universität Hamburg-Harburg, 21071 Hamburg, Germany

Abstract

Dense alumina-$TiAl_3$ composites with interpenetrating networks have been fabricated by reactive gas-pressure infiltration and squeeze casting of Al into sintered porous preforms containing 30 vol% TiO_2 and 70 vol% Al_2O_3. Strength of up to 543 ± 21 MPa with corresponding fracture toughness of $8{\cdot}6 \pm 0{\cdot}4$ MPa$\sqrt{m}$ and hardness of $H_{V10} = 565 \pm 27$ have been obtained. The present paper discusses processing parameters such as particle size of oxide precursor and preform porosity which control microstructural development and mechanical properties of the composites. © *1999 Elsevier Science Ltd. All rights reserved.*

Keywords: composites, microstructure-final, mechanical properties, $TiAl_3$, Al_2O_3, reactive infiltration.

1 Introduction

In the last decade, interpenetrating aluminum/ceramic composites have attained great attention due to their advanced damage tolerance and wear resistance. However, established conventional infiltration[1,2] and reactive processing routes for metal/ceramic composites such as directed metal oxidation[3] and reactive melt penetration[4,5] are essentially restricted to the manufacturing of Al-containing composites. For the fabrication of composites containing more refractory metals or intermetallics, uneconomically high temperature processing methods like gas-pressure infiltration, hot extrusion, hot pressing or HIP[6–10] are necessary. Recently, a novel P/M technique for the low-cost manufacturing of alumina-aluminide alloys (3A) has been developed.[11,12] The process involves the reaction sintering of attrition milled powder mixtures consisting of cheap raw materials like aluminum, metal oxides (e.g. TiO_2, Fe_2O_3, Nb_2O_5, ZrO_2, etc.) and/or elemental metals (Fe, Ni, Cr, Mo, etc.) to produce aluminide/alumina composites with interpenetrating networks. 3A materials exhibit low specific structural weight as well as good resistance to corrosion, wear and creep.

Similar materials can be fabricated by reactive infiltration as was indicated by squeeze casting Al into green bodies made of TiO_2 particles and whiskers.[13] However, reaction took place only partially and the resulting microstructures were inhomogenous. In a different approach, pressure infiltration of Al into presintered porous metal oxide bodies containing an Al_2O_3 network lead to dense and fully reacted composites.[14,15] For instance, TiO_2, Nb_2O_5, ilmenite ($FeTiO_3$) etc., were used as preforms to form Al_2O_3-matrix composites with interpenetrating networks of aluminides of Ti, Nb and (TiFe).

In this paper, the basic principles of fabricating i-3A composites will be reported, emphasizing gas-pressure infiltration and squeeze casting of Al into TiO_2-containing Al_2O_3 preforms. Processing parameters such as particle size and composition of preform powder oxides and preform porosity controlling microstructural development and mechanical properties are discussed.

2 Experimental Procedure

2.1 Composition and preparation of preforms

Powder mixtures containing 30 vol% TiO_2 and 70 vol% of three types of Al_2O_3 were ball milled for 3 h with 10 mm ZrO_2 (3Y-TZP) balls, rotovap dried and uniaxially pressed into plates with dimensions of $40 \times 50 \times 6\,mm^3$. Other oxides such as Nb_2O_5, ZrO_2, ilmenite, etc. were tested in a similar way. Subsequently, the green bodies were sintered in air using a heating rate of 3°C/min up to 1250°C with a hold for 30 min, finally the furnace was cooled at 10°C/min. Detailed property data of the preform

*To whom correspondence should be addressed.

are given in Table 1. Presintering of the green bodies proved to be useful because, first, reasonable mechanical stability during infiltration is provided by an Al_2O_3 network and, second, the open porosity fraction can be more precisely adjusted to a predetermined value which controls the final composition after infiltration. During infiltration, the following reaction occurs within the body:

$$3TiO_2 + 13Al \rightarrow 2Al_2O_3 + 3TiAl_3 \qquad (1)$$

The volume fraction of each phase in the final composition can be calculated by a volume balance, taking the specific molar volumes (V) of Al_2O_3, TiO_2, Al and the open porosity into account:

$$V^{p}_{Al_2O_3} + V_{TiO_2} + V_{pores} \overset{+V_{Al}}{\rightarrow} V^{p}_{Al_2O_3} + V^{s}_{Al_2O_3} + V_{TiAl_3} \qquad (2)$$

Where the indices p and s refer to primary Al_2O_3 contained in the preform and newly formed secondary alumina, respectively. $V^{p}_{Al_2O_3}$ remains constant and has no influence on the volume changes during reaction infiltration. The amount of $TiAl_3$ after reaction infiltration in the $TiAl_3/Al_2O_3$ composite can be calculated by

$$V_{TiAl_3} = V_{TiO_2} \cdot (1 - V_{pores}) \cdot \frac{V^{m}_{TiAl_3}}{V^{m}_{TiO_2}} \qquad (3)$$

2.2 Infiltration processes

For gas-pressure infiltration, the preforms were attached to a holder placed in a crucible and embedded into aluminum chips [Fig. 1(a)]. The infiltration furnace was heated to 850°C in vacuum using a heating rate of 10°C/min. After a 15 min hold, the argon gas-pressure was raised to 12 MPa at 2 MPa/min. In order to achieve complete infiltration, temperature and pressure were held for 10 min. Thereafter, the furnace was cooled to 660°C. The crucible with the metal bath was lowered by the hydraulic ram thereby lifting the samples out of the melt. Subsequently, the furnace was cooled to room temperature [Fig. 1(b)].

Die casting was performed by direct squeeze casting (Fig. 2). The preforms were heated to 900°C and inserted into the die preheated to 300°C. Liquid aluminum was filled into the die and the upper punch was immediately lowered squeezing the aluminum melt into the porous preform within <1 s. After solidification, the infiltrated preform was removed from the die. Some of the squeeze cast samples were tempered for 4 h in air at 640°C, hence just below the liquidus temperature of the aluminum to achieve complete reaction and homogenous and stoichiometric phase composition.

2.3 Sample characterization

Gas-pressure infiltrated and squeezed cast samples were cut into bars with dimension $4\times3\times40\,mm^3$. The surfaces were ground and diamond polished to 3 μm finish. Phase composition was characterized by X-ray diffraction (XRD) and microstructural development by scanning electron microscopy and optical microscopy, additionally, electron dispersive X-ray analysis was used. Fracture toughness (K_{IC}) was determined by indentation strength in bending[16] using a Vickers indenter with 10 kg load and modulus of rupture was measured in four point bending with 10/20 mm spans.

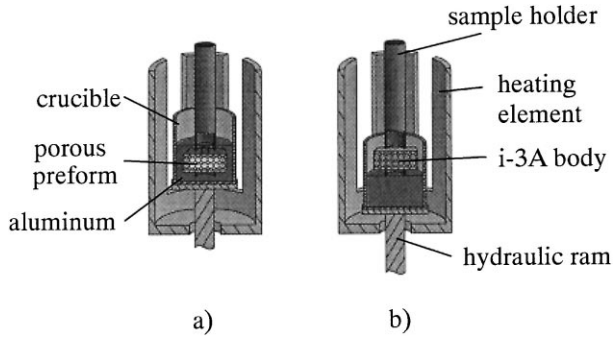

Fig. 1. Schematic of gas-pressure infiltration device.

Table 1. Characteristics of 30 vol% TiO_2/70 vol% Al_2O_3 preforms and properties of the resulting A1 reaction infiltrated composites

Sample	*Preform*		*Infiltrated composite*						
	Al_2O_3 grain size [μm]	*Density [%TD]*	*Al_2O_3 [vol%]*	*$TiAl_3$ [vol%]*	*Al [vol%]*	*Density [g/cm³]*	*Strength [MPa]*	*K_{IC} [MPa√m]*	*HV_{10} [GPa]*
F	0·5[a]	61·5	58·3	36·1	5·6	3·65	495 ± 15	5·0 ± 0·2	6·75 ± 0·25
M	5[b]	61·2	58·1	36·0	5·9	3·51	542 ± 21	8·6 ± 0·4	5·65 ± 0·27
C	15[c]	61·1	57·9	35·9	6·2	3·52	494 ± 95	6·6 ± 0·4	7·40 ± 0·48

[a] HPa 0,5, Condea, FRG.
[b] 5000, Alcoa, FRG.
[c] Gilox 63, Alcoa, FRG. TiO_2: Riedl de Haen, 41021, 0·5–1 μm, FRG.

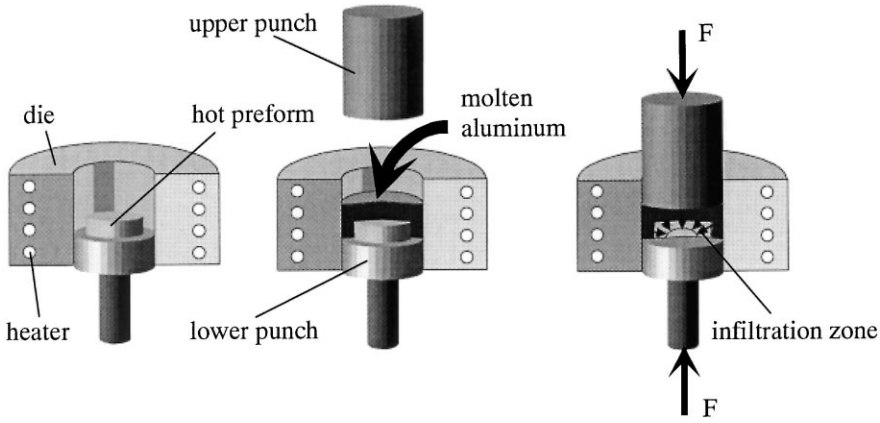

Fig. 2. Schematic of squeeze casting device.

3 Results and Discussion

3.1 Microstructure

The major phases of gas-pressure infiltrated Al_2O_3/TiO_2 preforms are $TiAl_3$, Al_2O_3 and Al (Fig. 3). The original TiO_2 can no longer be detected, indicating complete reaction with the aluminum melt to form $TiAl_3$ and Al_2O_3, corresponding to eqn (1). The presence of Al can be attributed to an additional open porosity within the preform caused by a phase transformation of TiO_2 from anatase to rutile during presintering as detected by XRD. The observed phase reaction is associated with a density change and thus with a change in volume ratio between open porosity and TiO_2. Taking this reaction into account, the final compositions of the preforms have been recalculated and are also listed in Table 1.

The typical microstructure of gas-pressure infiltrated i-3A composites is shown in Fig. 4. Both intermetallic/metal and ceramic phases are interpenetrating and a homogenous microstructure with no porosity is observed. In the fine grained composite F, primary and secondary Al_2O_3 (dark grey phase) can not be distinguished [Fig. 4(a)]. Both alumina phases are within the same size range. $TiAl_3$ (light grey) is homogeneously dispersed. The microstructure shows also some light areas corresponding to excess aluminum. In the coarse microstructure of composite C, the difference between primary and secondary alumina can be clearly distinguished. The large primary Al_2O_3 particles ($\sim 15\,\mu m$) are surrounded by small secondary particles in the range of $2\,\mu m$ with finely dispersed aluminide inclusions resulting from the reaction between Al and TiO_2.

The XRD pattern of squeeze cast samples in Fig. 5 shows that, during the short infiltration period, no aluminide formation took place. However, after

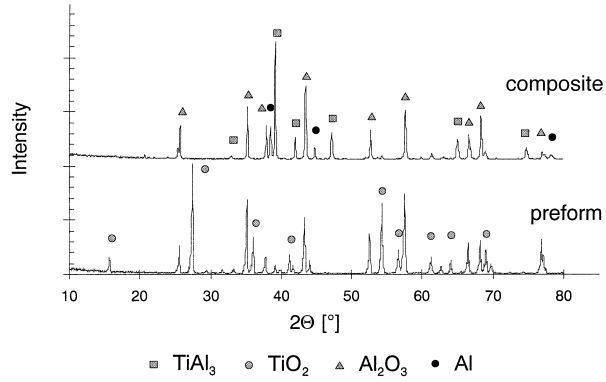

Fig. 3. XRD patterns of Al_2O_3/TiO_2 preform M and the resulting $Al_2O_3/TiAl_3$ composite M after gas-pressure reaction-infiltration.

annealing at 640°C for 4 h, TiO_2 can no longer be detected and new peaks, corresponding to $TiAl_3$ appear. Some remaining Al can also be detected. The as-cast microstructure [Fig. 6(a)] shows that the composite is dense, as in the case for gas-pressure infiltrated material, i.e. no pores are visible. After annealing, the composite phase composition changes drastically, but the microstructure remains dense and no pore formation is observed although the volume change on reacting is negative. The light grey phase usually associated with white Al inclusions is very fine-grained secondary Al_2O_3.

Comparing micrographs of gas-pressure infiltrated and squeeze cast composites, it is obvious that they are very similar, i.e. XRD patterns show comparable phase distributions. Hence, independently of the processing route, dense i-3A materials are obtained. Typical features of both infiltration processes are that, during infiltration, the shape of the preforms remains unchanged and no shrinkage occurs.

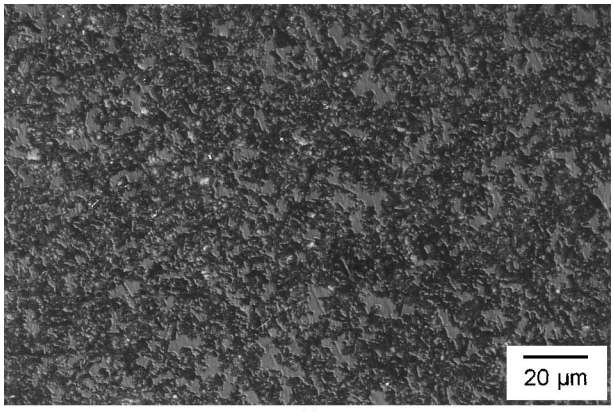

(a)

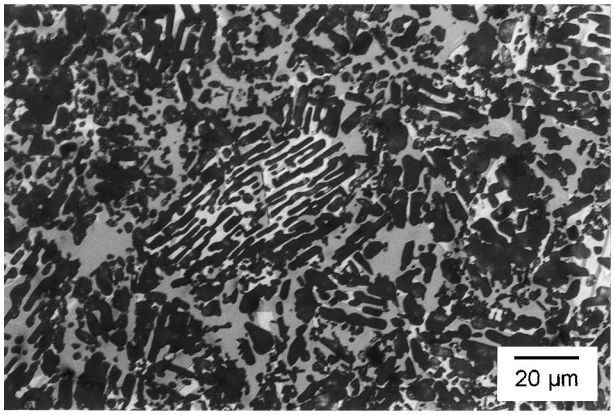

(b)

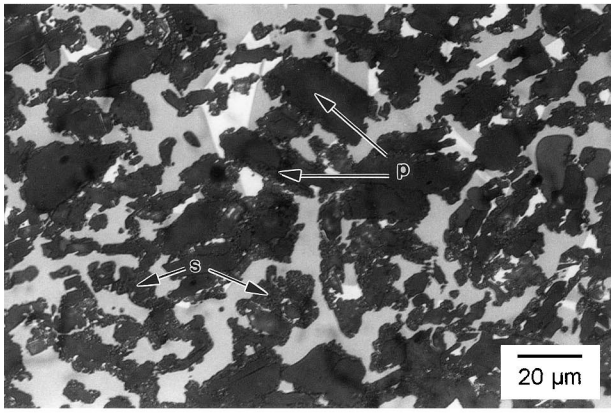

(c)

Fig. 4. Optical micrographs of gas-pressure infiltrated samples, (a) F, (b) M and (c) C (cf. Table 1). Al_2O_3 dark grey, $TiAl_3$ light grey and Al white. Figure 4(c), primary (p) and secondary (s) Al_2O_3 can easily be distinguished.

3.2 Mechanical properties

Preliminary mechanical properties of gas-pressure infiltrated $TiAl_3/Al_2O_3$ composites have shown fracture strengths of ~540 MPa (cf. Table 1) and fracture toughnesses of 8·6 MPa$\sqrt{m}$. The hardness of the composite increases with Al_2O_3 grain size and the strength rises with increasing dimensions of the metal phase. However, the composite C shows decreasing strength and toughness which can be caused by the very coarse grained primary Al_2O_3 acting as inhomogenous inclusion.

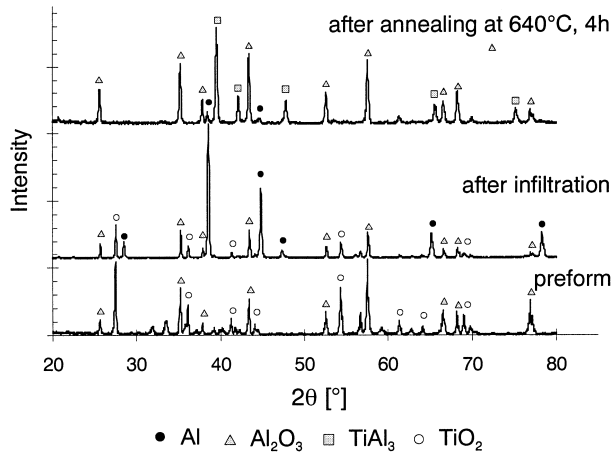

Fig. 5. XRD patterns of Al_2O_3/TiO_2 preform, and as squeeze cast and annealed composites.

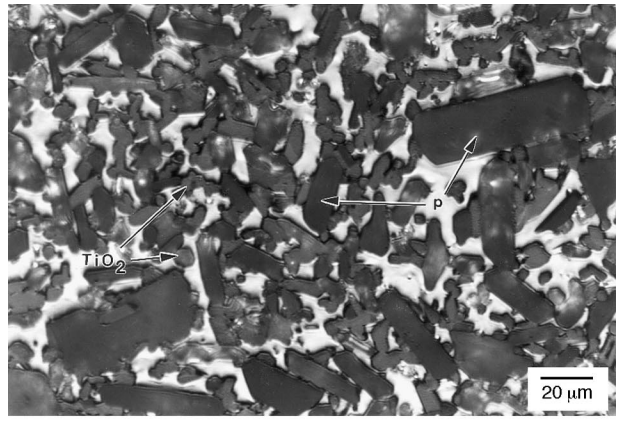

(a)

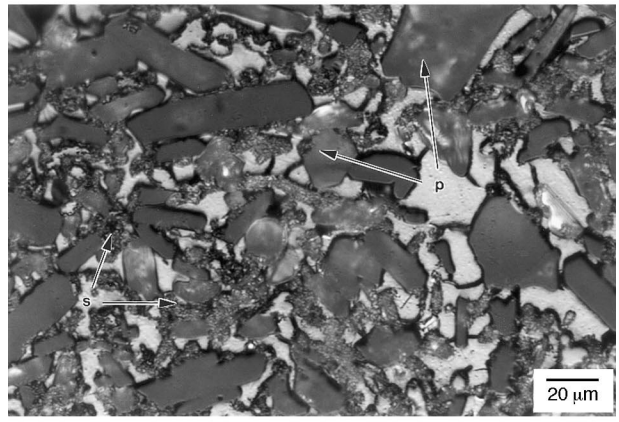

(b)

Fig. 6. Optical micrograph of (a) as squeeze cast and (b) annealed composites. Arrows indicate TiO_2 as well as primary (p) and secondary (s) Al_2O_3 the latter of which is intimately mixed with $TiAl_3$.

4 Conclusions

Dense and homogenous i-3A composites with interconnected Al_2O_3 and $TiAl_3$ networks have been fabricated by reactive infiltration of Al into porous Al_2O_3/TiO_2 preforms. It is interesting to note that this near net shape process generates composites with far higher melting temperatures than required for their fabrication. Since reaction

times are short, preform powders inexpensive and considerable flexibility in composition and microstructure tailoring exists, the i-3A process is very economical. It is obvious that the i-3A process is ideally suited for partial reinforcement of Al components.

References

1. Aghajanian, M. K., Rocazella, M. A., Burke, J. T. and Keck, S. D., The fabrication of metal matrix composites by a pressureless infiltration technique. *J. Mat. Sci.*, 1991, **26**, 447–454.
2. Asthana, R., Cast metal-matrix composites. I: Fabrication techniques. *J. Mat. Syn. Proc.*, 1997, **5**, 251–278.
3. Antolin, S., Nagelberg, A. S. and Creber, D. K., Formation of Al_2O_3/metal composites by the directed melt oxidation of molten aluminum–magnesium-silicon alloys; part I, microstructural development. *J. Am. Ceram. Soc.*, 1992, **75**(2), 447–454.
4. Breslin, M. C., Ringnalda, J., Seeger, J., Marasco, A. L., Daehn, G. and Fraser, H. L., Alumina/aluminium co-continuous ceramic composite (C4) materials produced by solid/liquid displacement reactions: processing kinetics and microstructures. *Ceram. Eng. Sci. Proc.*, 1994, **15**(4), 104–112.
5. Loehman, R. E., Ewsuk, K. and Tomsia, A. P., Synthesis of Al_2O_3-Al composites by reactive melt penetration. *J. Am. Ceram. Soc.*, 1996, **79**(1), 27–32.
6. Prielipp, H., Knechtel, M., Claussen, N., Streiffer, S. K., Müllejans, H., Rühle, M. and Rödel, J., Strength and fracture toughness of aluminum/alumina composites with interpenetrating networks. *Mat. Sci. and Eng.*, 1995, **A197**, 19–30.
7. Rankin, D. T., Stiglich, J. J., Petrak, D. R. and Ruh, R., Hot pressing and mechanical properties of Al_2O_3 with a Mo-dispersed phase. *J. Am. Ceram. Soc.*, 1971, **54**, 277–281.
8. Rödel, J., Prielipp, H., Claussen, N., Sternitzke, M., Alexander, K., Becher, P. and Schneibel, J. H., Ni_3Al/Al_2O_3 composites with interpenetrating networks. *Scr. Metall. et. Mater.*, 1995, **33**, 843–848.
9. Djali, P. D. and Linger, K. R., The fabrication and properties of nickel-alumina cermets. *Proc. Br. Ceram. Soc.*, 1978, **26**, 113–127.
10. Sun, X. and Yeomanis, J. A., Microstructure and fracture toughness of nickel particle toughened alumina matrix composites. *J. Mat. Sci.*, 1996, **31**, 875–880.
11. Claussen, N., García, D. E. and Janssen, R., Reaction sintering of alumina-aluminide alloys (3A). *J. Mater. Res.*, 1996, **11**, 2884–2888.
12. Schicker, S., García, D. E., Bruhn, J., Janssen, R. and Claussen, N., Reaction synthesized Al_2O_3-based intermetallic composites. *Acta mater.*, 1998, **46**, 2485–2492.
13. Fukunaga, H., Wang, X. and Aramaki, Y., Preparation of intermetallic compound matrix composites by squeeze casting. *J. Mat. Sci. Let.*, 1990, **9**, 23–25.
14. Wagner, F., Janssen, R. and Claussen, N., German patent DE 19605858, 16 February, 1996.
15. Scheu, C., Dehm, G., Kaplan, W. D., Wagner, F. and Claussen, N., Microstructure and phase evolution of niobium-aluminide-alumina composites prepared by melt-infiltration. *Phys. Stat. Sol.*, 1998, **166**, 241–255.
16. Bennision, R. F. and Lawn, B. R., Flaw tolerance in ceramics with rising crack-resistance behavior. *J. Mat. Sci.*, 1989, **24**, 3169.